PROTEINS
STRUCTURE ■ FUNCTION ■ BIOINFORMATICS

Mechanistic insight of photo-induced aggregation of chicken egg white lysozyme: The interplay between hydrophobic interactions and formation of intermolecular disulfide bonds

Jinbing Xie,[1,2] Meng Qin,[1,2]* Yi Cao,[1,2] and Wei Wang[1,2]*

[1] National Laboratory of Solid State Microstructure, Nanjing University, Nanjing 210093, China
[2] Department of Physics, Nanjing University, Nanjing 210093, China

ABSTRACT

Recently, it was reported that ultraviolet (UV) illumination could trigger the unfolding of proteins by disrupting the buried disulfide bonds. However, the consequence of such unfolding has not been adequately evaluated. Here, we report that unfolded chicken egg white lysozyme (CEWL) triggered by UV illumination can form uniform globular aggregates as confirmed by dynamic light scattering, atomic force microscopy, and transmission electron microscopy. The assembling process of such aggregates was also monitored by several other methods, such as circular dichroism, fluorescence spectroscopy, mass spectrometry based on chymotrypsin digestion, ANS-binding assay, Ellman essay, and SDS-PAGE. Our finding is that due to the dissociation of the native disulfide bonds by UV illumination, CEWL undergoes drastic conformational changes resulting in the exposure of some hydrophobic residues and free thiols. Subsequently, these partially unfolded molecules self-assemble into small granules driven by intermolecular hydrophobic interaction. With longer UV illumination or longer incubation time, these granules can further self-assemble into larger globular aggregates. The combined effects from both the hydrophobic interaction and the formation of intermolecular disulfide bonds dominate this process. Additionally, similar aggregation behavior can also be found in other three typical disulfide-bonded proteins, that is, α-lactalbumin, RNase A, and bovine serum albumin. Thus, we propose that such aggregation behavior might be a general mechanism for some disulfide-bonded proteins under UV irradiation.

Proteins 2011; 79:2505–2516.

Key words: UV illumination; granular aggregate; protein misfolding; hydrophobic collapse; disulfide bridging.

INTRODUCTION

Proteins require correctly folded structures to perform their particular biological functions.[1–4] Harsh solvent conditions (such as high temperature, low pH, or the presence of denaturants) or mutations in their sequences,[5–8] can cause proteins to undergo structural transition and give rise to amyloid-like fibrils. Such protein aggregations are tied to a number of fatal diseases, such as Alzheimer's and Parkinson's.[9–15] Moreover, pathogenesis studies on neurodegenerative diseases (e.g., Alzheimer's) suggested that instead of the final fibrillar aggregates, the granular aggregates formed at the early aggregation process is the leading factor for these diseases, owing to their high reactivity with a wide range of cellular components.[16–18] Additionally, it was recently found that the globular aggregates formed by partially unfolded proteins are also related to some diseases, such as Lewy body associated disorders.[19,20] Therefore, investigating the dynamic change in the morphology and aggregation of proteins is of great importance for the evaluation of the impact of harsh conditions on proteins, as well as the pathogenesis of the related diseases.

Previously, we have reported that ultraviolet (UV) illumination can trigger the unfolding of chicken egg white lysozyme (CEWL; schematic picture shown in Fig. 1) under physiological condition, which has also been observed in other disulfide-bonded proteins[21–26] and even developed into powerful biotechnological tools for protein immobilization.[27] Such unfolding process of the proteins is quite different from the traditional denaturing processes induced by disrupting the noncovalent interactions in the tertiary structures as it is solely initialized by rupturing the native

Grant sponsor: National Basic Research Program of China; Grant number: 2007CB814806; Grant sponsor: National Natural Science Foundation of China; Grant numbers: 10904064, 10834002, 11074115; Grant sponsor: Natural Science Foundation of Jiangsu Province of China; Grant number: BK2009008
*Correspondence to: Meng Qin, National Laboratory of Solid State Microstructure, Nanjing University, Nanjing 210093, China. E-mail: qinmeng@nju.edu.cn or Wei Wang, National Laboratory of Solid State Microstructure, Nanjing University, Nanjing 210093, China. E-mail: wangwei@nju.edu.cn.
Received 25 January 2011; Revised 21 April 2011; Accepted 26 April 2011
Published online 10 May 2011 in Wiley Online Library (wileyonlinelibrary.com).
DOI: 10.1002/prot.23074

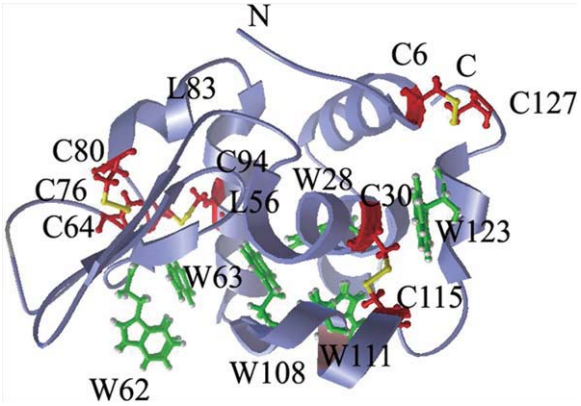

Figure 1

The schematic structure of CEWL. It contains six tryptophan (Trp) residues marked with green color and eight cysteine (Cys) residues (red color) forming four native disulfide bonds (yellow color), that is, Cys6-Cys127, Cys30-Cys115, Cys64-Cys80, and Cys76-Cys94, respectively. There are six hydrophobic clusters with the maximal hydrophobicity around the residues cysteine 6, tryptophan 28, leucine 56, leucine 83, tryptophan 108, and tryptophan 123, respectively.

disulfide bonds through a tryptophan/tyrosine based photochemical process. In traditional chemical denaturing experiments, many proteins have the ability to resume their native state upon removing the chemical denaturants. Thus the questions arise, can these "special" unfolded CEWL molecules resume their native fold and reform their native disulfide bonds during or after UV irradiation? Or alternatively, do these unfolded CEWL molecules aggregate into special structures? Investigation the self-assembly and aggregation of photo-induced unfolded CEWL molecules under UV illumination will also be of great practical significance in understanding the damage of UV light to proteins.

In this work, we disclose that under strong UV illumination (200 μW/cm^2), CEWL can promptly unfold and self-assemble into aggregates in granular shape without resuming its native fold. These granules are very active and can further assemble into larger globular aggregates when the UV illumination time is prolonged. It is quite different from the fibrillar aggregates of lysozyme formed under harsh conditions or by introducing destabilizing mutants even under native condition.[28,29] Based on the detailed characterization of the unfolded CEWL molecules under UV illumination and the morphologies of the aggregates during the UV illumination process, we propose a mechanism that may account for such unique aggregation behavior. CEWL partially unfolds under UV illumination with some hydrophobic residues and free thiols exposed, due to the rupture of disulfide bonds. The interplay between the hydrophobic interaction and the intermolecular disulfide bonding governs the aggregation of CEWL. Importantly, similar aggregation behavior can also be found in other three typical disulfide-bonded proteins, that is, α-lactalbumin, RNase A, and bovine serum albumin (BSA). Because disulfide bond containing proteins are ubiquitous in nature and can be engineered artificially,[30–32] we anticipate that such aggregation behavior can be extended to other disulfide-bonded proteins that are sensitive to UV illumination.

MATERIALS AND METHODS

Chemicals

CEWL, bovine α-lactalbumin, RNase A, 1-anilinonaphthalene 8-sulfonate (ANS), Thioflavin T (ThT), and 5, 5 P-dithiobis (2-nitrobenzoic acid) (DTNB, Ellman's reagent) were purchased from Sigma. BSA was purchased from Roche. Except chymotrypsin (sequencing-grade), all other chemical reagents used in our experiments are of analytical grade without further purification. A total of 0.02*M* phosphate buffer ((NaH_2PO_4 and Na_2HPO_4) at pH 7.0 was used for all experiments, except for the Ellman assay and chymotrypsin digestion.

UV illumination

CEWL (2 mg/mL) in sealed 10 mm × 10 mm quartz cuvettes was illuminated by the UV-B lamp (Ziguang Company, China) with wavelength centered at ~285 nm. Note that both tryptophan and tyrosine residues can be excited under such bandwidth of UV wavelength. The light intensity was measured by the optical power meter (818-ST-UV/DB- 840C, Newport). We did not stir the solution during illumination.

Atomic force microscopy (AFM)

An aliquot of about 10 μL sample was placed on a newly peeled mica wafer for about 15 min, and then rinsed with 50 μL of Milli-Q water to remove unattached proteins and salts. The sample on the mica surface was dried at room temperature before the images were taken. AFM images were obtained by scanning the mica surface using a Nanowizzard II AFM (JPK, Berlin, Germany) operating in a tapping mode (conditions: scan rate, 0.8 Hz; resonant frequency range of AFM tips, 200–497 kHz; tip radius, 5 nm; number of pixels, 512 × 512).

Transmission electron microscopy (TEM)

In this study, the lysozyme sample (2 mg/mL) for the TEM measurement was illuminated for 72 h, and macroscopic aggregates can be found on the bottom of the cuvette. Thus, we only used the supernatant of the sample for TEM measurement. The concentration of this sample is lower than the original 2 mg/mL due to the formation of macroscopic aggregates. About 15 μL supernatant of the illuminated CEWL solution was placed on a copper

grid (300-mesh) covered by a carbon-coated collodion film for about 5 min. The sample was further negatively stained with 20 μL of 2% (w/v) phosphotungstic acid solution for about 60 s. The image was taken using a Hitachi H-7650 transmission microscope with an acceleration voltage of 80 kV.

Dynamic light scattering (DLS)

The mean particle size of the aggregates was obtained by DLS method using a Brookhaven BI-200SM system (Brookhaven). All DLS measurements were carried out using a wavelength of 640.0 nm at room temperature.

Circular dichroism (CD)

CD spectra were obtained by using Jasco J-810 spectrophotometer (Tokyo, Japan) under constant nitrogen flush at 25°C. The concentration of CEWL is 2.0 mg/mL for the preparation of UV induced aggregates. The near-UV CD spectra of proteins (2.0 mg/mL) were collected between 250 nm and 300 nm with a 10 mm light-path. Due to the requirement of the sample concentration for the far-UV CD spectrum which was recorded from 190 nm to 250 nm with a 1 mm light-path, we diluted the illuminated sample (2.0 mg/mL) to 0.2 mg/mL. Each time, five scans were averaged to increase the signal-to-noise ratio of the measurements.

Fluorescence spectroscopy

The concentration of CEWL is 2.0 mg/mL for the preparation of UV induced aggregates. For the measurement requirement of fluorescence spectroscopy, the illuminated sample was diluted to 0.036 mg/mL. The measurement was taken using fluorescence spectrophotometer (Jasco FP-6500) with 10 mm light path at room temperature. The excitation wavelength was 285 nm, and the emission spectra were measured from 295 to 450 nm. Additionally, the bandwidths of excitation and emission slits were set as 3 nm and 5 nm, respectively.

ANS-binding assay

The hydrophobic probe dye 1-anilino-naphthalene 8-sulfonate (ANS) was used to investigate the exposure of the hydrophobic residues. The concentrations for the protein samples (native and illuminated CEWL) and ANS are 2.0 mg/mL and 100 μM, respectively. After 30 min incubation under dark condition, the emission spectra at 480 nm of the samples were measured by fluorescence spectrophotometer (Jasco FP-6500) with the excitation wavelength at 398 nm. The bandwidths of excitation and emission slits were set as 3 nm and 5 nm, respectively.

SDS-PAGE

Illuminated samples were analyzed by SDS-PAGE under normal and reducing conditions. For the case of normal condition, samples were mixed with laemmli sample buffer. For the case of reducing condition, 10% β-mercaptoethanol was added before the mixture with laemmli buffer. All samples were heated at 100°C for 10 min in Tris/glycine buffer (pH 8.8) containing SDS. After electrophoresis, the gels were stained by Coomassie Blue for 30 min and destained for 4 h on a table-top rocker.

Ellman assay

Free thiol groups were detected with the Ellman assay upon reaction with the sulfhydryl reagent DTNB. Illuminated CEWL (110 μL, 2 mg/mL) was mixed with DTNB (1.9 mL, 1 m*M*) solution and the absorbance at 412 nm was subsequently measured by UV/VIS spectrophotometer (Jasco, V-550).

Mass spectrometry

The thiol groups in the illuminated CEWL sample were carbamidomethylated by adding an equal volume of 10 m*M* iodoacetamide in 0.02*M* phosphate buffer (pH 7.0), and allowed the reaction to proceed for about 45 min in dark condition at room temperature. Both of the original and illuminated CEWL samples were resuspended in 100 m*M* Tris-HCl with $CaCl_2$ and then chymotrypsin was added with a 1:50 ratio (w:w). The mixtures were incubated for 18 h at room temperature. The resulted peptide mixtures were subjected to quadrupole fourier transform ion cyclotron resonance mass spectrometry (Q-FTICR-MS) and the intact proteins were analyzed on the matrix assisted laser desorption/ionization time-of-flight mass spectrometry (MALDI-TOF-MS).

RESULTS

The morphology of CEWL aggregates triggered by UV illumination

We applied UV illumination to the CEWL samples with an intensity of 200 μW/cm^2 at room temperature, and the aggregates were monitored in real time by DLS. As shown in Figure 2(A), CEWL started to form observable aggregates of diameters ~30 nm after 10 min of illumination. The size of the aggregates grew monotonically with the increase of illumination time and reached diameters ~80 nm and ~150 nm after 30 and 50 min of illumination, respectively. Then, the detailed morphology of the aggregates was investigated by AFM. As shown in Figure 2(B), after illumination for 30 min, CEWL formed small round-shaped granular aggregates with diameter of ~40 nm and height around 25 nm. Comparing with the size of folded CEWL (~5 nm), we estimated that the

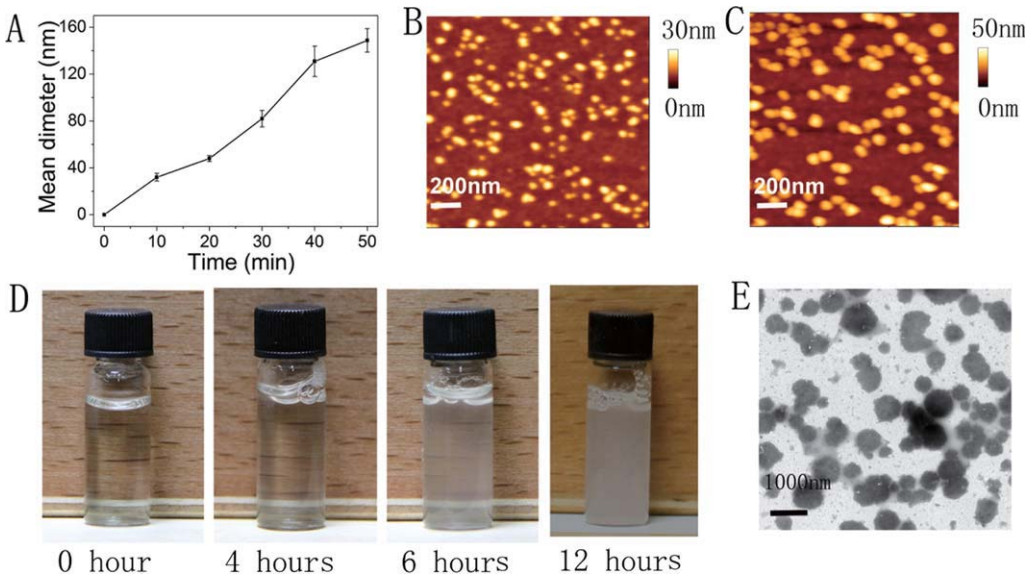

Figure 2

The morphology of the CEWL aggregates on UV illumination (The concentration of CEWL is 2 mg/mL, and the intensity of UV light is 200 μW/cm^2.) (**A**) The change of the size of the aggregate in the first hour on UV illumination is monitored by DLS. AFM images of the aggregates under (**B**) 0.5 and (**C**) 1 h of illumination. (**D**) The photographs of the CEWL samples under different illumination times, that is, 0 h, 4 h, 6 h, and 12 h. After 6 h or longer illumination, the CEWL solution becomes turbid, indicating the formation of macroscopic aggregates. (**E**) TEM image of the spherical aggregates in the supernatant of the CEWL sample under 72 h continuous illumination.

granular aggregates are formed by ~300 CEWL molecules. As shown in Figure 2(C), the diameter and height of granular aggregates increase to ~75 and ~45 nm, respectively, when the illumination time is increased to 60 min. Thus, the size of the CEWL aggregates revealed by AFM is consistent with that observed by DLS. Note that besides isolated globular aggregates, we also observed the oligomerization of individual granular aggregates. When the illumination time is further prolonged to 6 h or longer, macroscopic aggregates are obviously observed in the CEWL samples [Fig. 2(D)]. The longer the illumination time, the more opaque the solution is. Formation of inter-sphere aggregates may be the sole mechanism that accounts for such macroscopic aggregation. It is of noting that not all the proteins in the solution form macroscopic aggregates. Even after 72 h of continuous UV illumination, we still observed spherical aggregates of ~800 nm in the supernatant by TEM, as shown in Figure 2(E). This is a clear evidence that the macroscopic aggregation is indeed from the growth of the spherical aggregates.

UV illumination induces partially unfolding of CEWL with the exposure of hydrophobic residues

After characterizing the morphology of the CEWL aggregates, we then studied the mechanism of the aggregation process. We first investigated the structural changes of CEWL in the aggregates on UV illumination by using far-, near-UV CD, and fluorescence spectroscopy. As shown in Figure 3(A), far-UV CD spectrum of native CEWL presents two characteristic negative peaks at 208 nm and 222 nm, consistent with the typical α-helical structure of CEWL. However, on illumination these two peaks increased dramatically, indicating that CEWL was partially unfolded and gradually lost its secondary structures. The longer the illumination, the less the secondary structures remained in the sample. However, it is worth noting that no obvious β-sheet structure or random coil appeared in the CD spectra even after 12 h of illumination. This is different from the change of tertiary structure of CEWL on illumination. As the CEWL molecules partially retain their secondary structures and dramatically lose their tertiary structure, we define such state of CEWL molecules as partially unfolded state. We also applied the intrinsic tryptophan fluorescence of CEWL to probe the structural changes of CEWL along the illumination process. Instead of changing monotonically, the intensity of tryptophan fluorescence first increased slightly and then decreased significantly to a value much lower than the original one with an obvious red shift of its peak position from 330 nm to ~350 nm. As tryptophan fluorescence is very sensitive to local chemical environment of proteins, this also indicates that the tertiary structure of CEWL undergoes dramatic disruption during the illumination process, consistent with the CD observations.

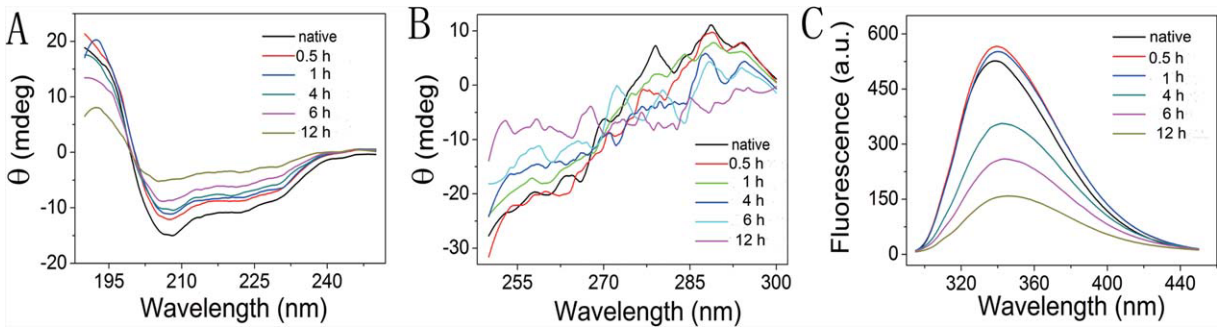

Figure 3

Structural characterization of native and illuminated CEWL. (**A**) far-UV and (**B**) near-UV CD spectra; (**C**) fluorescence spectra. The CEWL samples (2.0 mg/mL) were illuminated by UV light with an intensity of 200 μW/cm^2 for 0.5 h, 1 h, 4 h, 6 h, and 12 h, respectively.

Previous studies have found that there are six hydrophobic cores in CEWL, which are tightly buried inside its native conformation.[33–38] The disruption of the tertiary structure in harsh conditions could expose these inner buried hydrophobic residues, providing a critical driving force for the self-assembly process. To confirm whether the UV illumination can also lead to the exposure of hydrophobic residues, we used 8-anilino-1-naphthalene sulfonate (ANS) fluorescence, a reagent highly sensitive to the hydrophobic environment, as a probe to detect the change of the hydrophobicity of CEWL during the UV illumination.[39] As shown in Figure 4(A), the fluorescence intensity of ANS at 480 nm in the UV illuminated samples increases rapidly with the illumination time and reaches a value ~100 a.u. at 12 h. This indicates that lots of buried hydrophobic residues in native CEWL are certainly exposed to the solvent during continuous UV illumination.

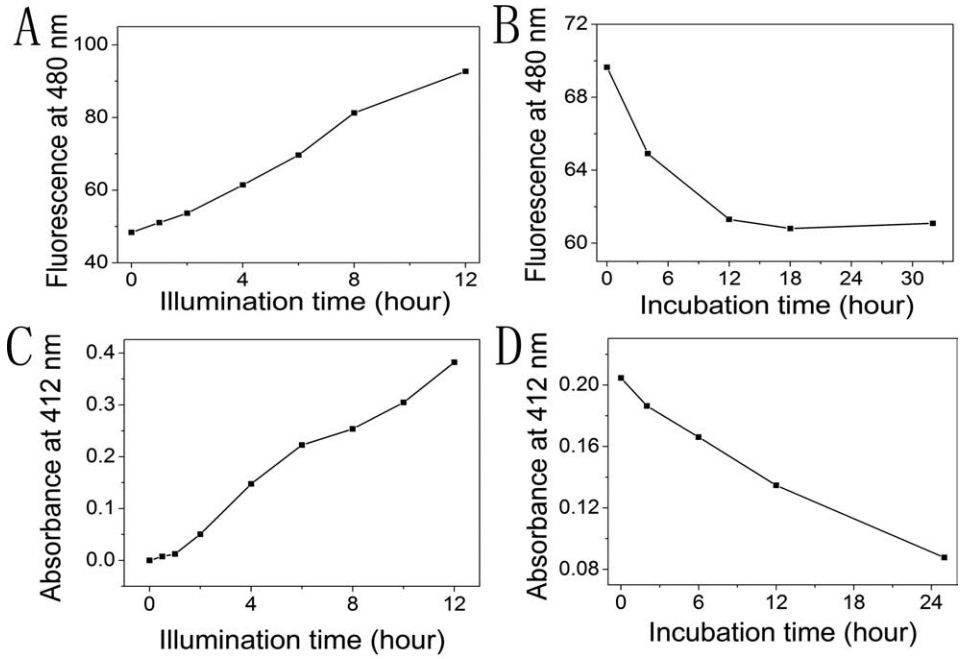

Figure 4

The changes of ANS (100 μM) fluorescence intensity at 480 nm of CEWL (2.0 mg/mL) as functions of (**A**) illumination time and (**B**) incubation time after 6 h continuous UV illumination. The absorption spectra at 412 nm of CEWL with the addition of DTNB as functions of (**C**) illumination time and (**D**) incubation time after 6 h illumination.

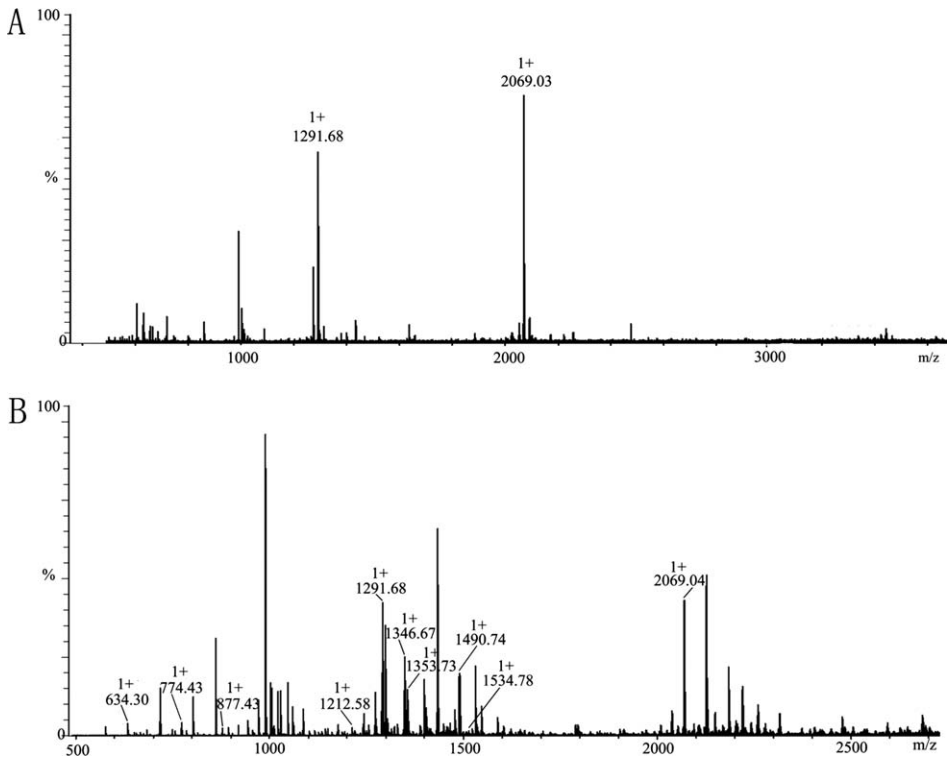

Figure 5

Q-FT-ICR mass spectra of the peptide fragments of (**A**) native and (**B**) illuminated CEWL under chymotrypsin digestion, respectively. Before digestion, carbamidomethylation was added to protect the free thiols. The peaks of important digested products are marked in detail and the related peptide fragments and their containing disulfide bonds or thiols are listed in Table I.

Breakage of native disulfide bonds is the sole reason for the partially unfolding of CEWL

How does CEWL reach the partially unfolded state on UV illumination? Native CEWL is largely stable with a thermodynamic stability of 10.2 kcal/mol.[40] Structural studies emphasize the importance of these disulfide bonds to the stabilization of native CEWL structure. All the four disulfide bonds in native CEWL are buried inside, which are inaccessible by the reducing agent in solvent.[41,42] As reported previously, UV illumination allowed the reduction of disulfide bonds in CEWL via a tryptophan/tyrosine based photochemistry process.[21–26] Here, we observed that such reduction of disulfide bonds could dramatically disturb the tertiary structure of CEWL and resulted in the further aggregation. To elucidate which disulfide bonds are prone to disruption on UV illumination and whether the free thiols from the ruptured disulfide bonds contribute to the aggregation process, we resorted to the Ellman assay and chymotrypsin digestion based mass spectroscopy. We first used Ellman assay to quantitatively monitor the amount of free thiols in CEWL under illumination.[43] We added sulfhydryl reagent 5, 5 p-dithiobis (2-nitrobenzoic acid) (DTNB) to the illuminated CEWL solution. DTNB can react with free thiols in solution and release TNB^-, which has a characteristic UV absorbance peak at 412 nm. As shown in Figure 4(C), on illumination, the quantity of free thiols in the sample increases gradually as indicated by the rise of absorbance intensity at 412 nm and reaches a maximum ~0.382 after 12 h of illumination. These free thiols must be produced from the reduction of native disulfide bonds, and the amount of free thiols is about 3.65 per CEWL molecule on average.

We then used chymotrypsin digestion and mass spectroscopy to investigate the detailed breakage and reformation of disulfide bonds in CEWL. Chymotrypsin is a protease that digests peptide bonds after sequence residues tyrosine (Y), leucine (L), tryptophan (W), phenylalanine (F), and methionine (M).[44] The presence or absence of the disulfide bonds can be revealed from the mass of the digested fragments. The mass spectra of the chymotrypsin digested products for the native CEWL and illuminated one are shown in Figure 5(A,B), respectively. Clearly, more peaks are displayed in the mass spectra of digested sample [Fig. 5(B)], which corresponds to the peptide fragments containing free thiols by the reduction of native disulfide bonds or the non-native disulfide bonds by these newly generated thiols. The detailed results of the free thiols and disulfide bonds

Table I
Masses of Peptides Derived from CEWL after Digestion with Chymotrypsin

Mass (Da)	Positions	Disulfide bond or Cys	Peptide sequence
634.30	4–8	C6	GR***C***EL
774.43	124–129	C127	IRG***C***RL
877.43	76–83	C80	CNIP***C***SAL
1346.67	64–75	C64	***C***NDGRTPGSRNL
1490.74	112–123	C115	RNR***C***KGTDVQAW
1212.58	4–8	C6–C30	GRCEL
	29–34		VCAAKF
1291.68	4–8	C6–C127	GRCEL
	124–129		IRGCRL
1353.73	29–34	C30–C127	VCAAKF
	124–129		IRGCRL
1534.78	76–83	C80–C127	CNIPCSAL
	124–129		IRGCRL
2069.04	29–34	C30–C115	VCAAKF
	112–123		RNRCKGTDVQAW

The italics "***C***" in bold correspond to the carbamidomethylated Cys residues. The masses of peptide fragments with a carbamidomethylated thiol can be calculated by adding 57.5 Da.

containing in the digested peptide fragments are listed in Table I by analyzing the mass spectra of the native CEWL and illuminated one. In detail, the peaks at 634.30, 774.43, 877.43, 1346.67, and 1490.74 Da correspond to the carbamidomethylated peptide fragments that contain free thiol groups of Cys6, Cys127, Cys80, Cys64, and Cys115, respectively. Besides these fragments containing free thiols, we also detected many fragments with native or non-native disulfide bonds, indicating that the free thiols are highly reactive. For example, we found that the Cys127 can reform native or non-native disulfide bonds with almost all other free thiols (Cys6-Cys127, Cys30-Cys127, and Cys80-Cys127). This might be caused by high flexibility of the C-terminal fragment that can facilitate residue Cys127 to approach other thiols and promote the formation of disulfide bonds. The similar behavior is also found for the N-terminal Cys6. As the disulfide bonds play extremely important roles in stabilizing the protein's tertiary structure, the rupture of disulfide bonds in CEWL can result in the disruption of the compact native structure and promote the exposure of buried hydrophobic residues.

Granular aggregates are formed mainly by hydrophobic aggregation among partially unfolded CEWL

As discussed above, the breakage of native disulfide bonds under UV illumination can lead to the partial unfolding of CEWL and the exposure of lots of hydrophobic residues. Thus, these exposed hydrophobic residues can rapidly self-assemble into granules as observed in Figure 2(B,C). However, besides the hydrophobic interactions, it is important to make clear whether the non-native intermolecular disulfide bonds formed by the exposed thiols also participate in the aggregation process. If these free thiols in the partially unfolded CEWL molecules form intermolecular disulfide bonds, they could be revealed by SDS-PAGE. This is because the intermolecular disulfide bonds are quite different from those intramolecular native ones, which can lead to the formation of CEWL oligomers. However, in the gel (Fig. 6), only monomers (~14 kD) are observed in lane 6 when the CEWL sample was illuminated for 30 min. This reveals that the granules [Fig. 2(B)] formed in the early stage of illumination are almost dominated by the hydrophobic interactions without much participation of intermolecular disulfide bonds. This is because that at the initial stage of UV illumination, the destruction of tertiary structure exposes lots of buried hydrophobic residues to the surface. Meanwhile, still a lot of secondary structures are retained, hindering the formation of intermolecular disulfide bonds due to the lack of sufficient chain flexibility. More importantly, in our system, the only oxidant, dissolved oxygen, is presented in low quantity, making the formation of disulfide bonds a much slower process than the hydrophobic interactions.

The self-assembling process of larger globular aggregates is controlled by intermolecular disulfide bonds and hydrophobic stacking among granules

During the illumination process, there are two different phases in the change of hydrophobicity. The unfolding of CEWL exposes hydrophobic residues, which causes the increase of hydrophobicity and induces the formation of granules. However, the formation of granular aggregates allowed the exposed hydrophobic residues to be

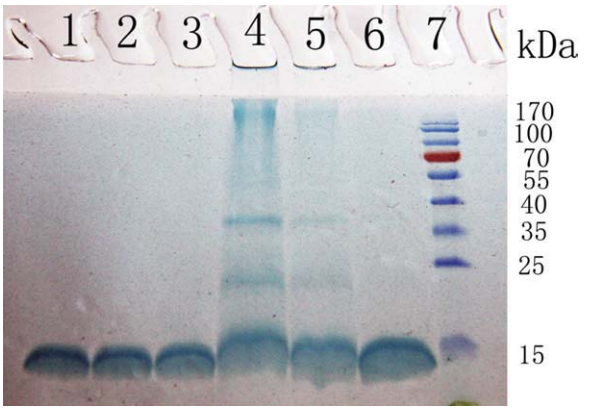

Figure 6
The SDS-PAGE analysis of intermolecular disulfide bonds for the aggregates of CEWL with different illumination time. Lanes 4, 5, and 6 correspond to the CEWL samples under 12, 6, and 0.5 h of illumination, respectively. The reduced samples corresponding to these lanes are shown in lanes 1, 2, and 3, respectively. Lane 7 is the protein marker. [Color figure can be viewed in the online issue, which is available at wileyonlinelibrary.com.]

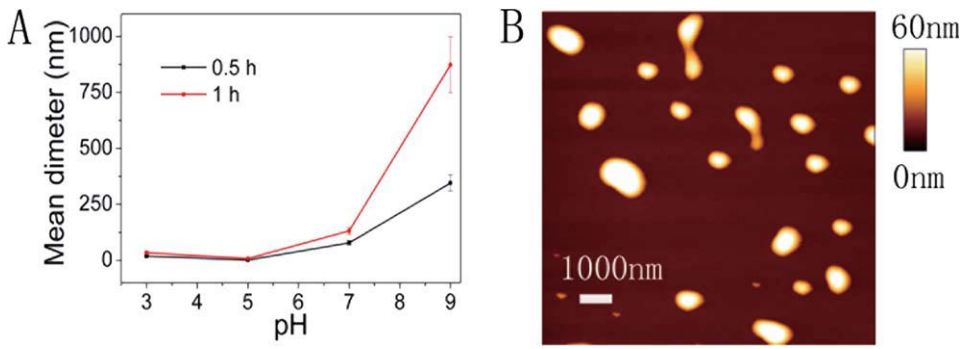

Figure 7

(**A**) The size of CEWL aggregates under 0.5 (black line) and 1 h (red line) UV illumination at different pH conditions are monitored by DLS. (**B**) The large aggregates (~1 μm in diameter) under 1 h of illumination at pH 9 are displayed in AFM image. The concentration of CEWL sample is 2 mg/mL and the intensity of UV light is 200 μW/cm^2.

buried and leads to the decrease of hydrophobicity. In fact, the continuous increase of hydrophobicity of CEWL during the illumination process as shown in Figure 4(A) indicates that there are also many hydrophobic residues exposed on the surfaces of the aggregated granules. Thus, these granules have great capability to interact with each other or with neighboring partially unfolded CEWL molecules. These observations allow us to infer the formation mechanism of granular aggregates as seeds to further aggregate into larger globular aggregates. Furthermore, when the illumination of UV light is switched off after 6 h, the ANS intensity of the illuminated sample decreases rapidly and reaches a minimum of ~60 a.u. after about incubation for 10 h [Fig. 4(B)]. This means these larger globular aggregates reach to a stable state with most of the hydrophobic residues buried. Additionally, during this stage, the formation of intermolecular disulfide bonds also plays critical roles in the growing and stability of larger globule-like aggregates. As shown in Figure 6, when the illumination time is prolonged to 6 h, a lot of dimmer, trimer and other higher molecular weight multimers are observed in lane 5 and disappeared in lane 2 by adding excessive reducing agents β-mercaptoethanol. Moreover, when we prolong the illumination time to 12 h, there are significant amount of multimers of CEWL in the illuminated sample as shown in lane 4, which will also disappear in lane 1 with the addition of excess β-mercaptoethanol. Moreover, incubation can also lead to more pronounced intermolecular disulfide bonds. As evidenced from the Ellman assay [Fig. 4(D)], the absorbance of DTNB at 412 nm dropped from 0.20 a.u. to 0.09 for a CEWL sample after incubation for 25 h.

DISCUSSION

In this work, we investigated the mechanism of CEWL aggregation on UV illumination in the native condition. Under the appropriate illumination intensity, CEWL molecules assemble into granular aggregates and subsequently, larger globular aggregates with prolonged illumination time or incubation time. We attribute this to the unique nature of partially unfolded CEWL molecules, which are composed of many free thiols and solvent exposed hydrophobic residues, making them prone to forming intermolecular aggregations. Thus, the two main driving forces, hydrophobic interactions and disulfide bridging, control the aggregation process. At the early stage of UV illumination, the formation of granules is solely determined by the hydrophobic interaction without much participation of intermolecular disulfide bonds. This is because most of the secondary structures are still retained at a so-called metastable partially unfolded state, although most of the tertiary structures of CEWL molecules are disrupted. At this state, the secondary structure remains stable for a certain time period without the sudden aggregation of the CEWL molecules at the macroscopic level. Additionally, such structural rigidity also inhibits the reaction of intermolecular free thiols to form disulfide bonds in such a short time under a weak oxidative condition. Due to the above-mentioned reasons, the granular aggregates formed at the early stage are mainly through hydrophobic interactions. Note that these granular aggregates are highly reactive because they still contain many free thiols and solvent exposed hydrophobic residues. We found that both the prolongation of illumination time and the additional incubation process can cause dramatic increase of the size of the aggregates due to further aggregation of these granules. Additionally, during this stage, the intermolecular disulfide bonds play critical roles in the growing of CEWL aggregates from small granules to larger globular aggregates. In fact, such aggregation behavior is quite sensitive to the pH condition of protein concentration. The size of lysozyme obviously increases when the sample solution changes from acidic condition to alkaline condition (Fig. 7).

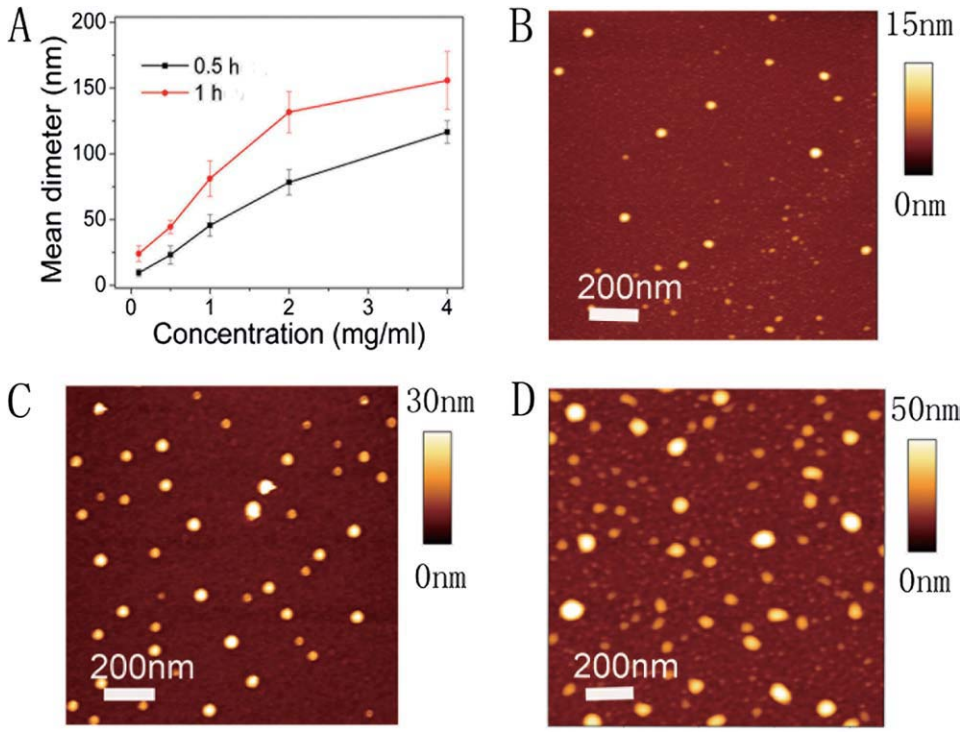

Figure 8

(**A**) The change of the size of CEWL aggregates monitored by DLS on 0.5 h (black line) and 1 h (red line) UV illumination as a function of protein concentration. The typical AFM images of CEWL aggregates (on UV illumination for 1 h at pH 7) at different concentrations are shown in (**B**) 0.5 mg/mL, (**C**) 1.0 mg/mL, and (**D**) 4.0 mg/mL, respectively. The intensity of UV light is 200 μW/cm^2.

Additionally, under same illumination condition, the size of the aggregates is also dependent on the concentration of proteins and it grows accordingly with the increase of concentration as shown in Figure 8. Therefore, by changing the solvent conditions and protein concentration, it is possible to adjust the interplay between hydrophobic interactions and disulfide bonding and thus control the aggregation behavior of CEWL.

It is worth noting that the CEWL in the granular aggregates are partially unfolded with lots of native secondary structures maintained, instead of immediately forming amyloid-like β-structures.[45–48] It was found that human lysozyme, a structural homolog of CEWL, formed amyloid-like fibrillar aggregates after partially unfolding. In their studies, human lysozyme was destabilized by undergoing harsh solvent condition or introducing sequence mutants in native condition with their disulfide bonds retained.[29,49,50] By comparison, in our study, the native disulfide bonds are directly reduced under native condition by inner excitations of tryptophan and tyrosine residues, which can dramatically destroy the stability of tertiary structure of CEWL exposing the buried hydrophobic residues. However, such alteration cannot eliminate all of the secondary structures dominated by the inner hydrogen bonds but not the disulfide bridges. Thus, although it allows the formation of inter- or intra-molecular non-native disulfide bonds, the reduction of chain flexibility makes the formation of intermolecular β-sheet not structurally feasible. This may be the sole reason for the partially unfolded structure of CEWL in the aggregates.

Moreover, we studied the detailed chemistry of such metastable partially unfolded state. We found that in such state, at least three out of four disulfide bonds have been disrupted on illumination. As mentioned in previous studies, the distance between the native disulfide bond and the nearby tryptophan/tyrosine residues is a key factor for the rupture of the native disulfide bonds induced by UV illumination.[51] In the native conformation of CEWL, the nearest distances between the tryptophan side chains (Trp 111 and Trp 123) and the disulfide bond Cys30-Cys115 are only 5.37 and 7.49 Å, respectively. Thus, the disulfide bond Cys30-Cys115 can be reduced with high probability by the electrons transfer from Trp 111 and Trp 123 under UV illumination. Similarly, it is also observed that the native disulfide bonds Cys6-Cys127 and Cys64-Cys80 have been reduced under UV illumination. The reduction of these disulfide bonds offers CEWL molecule significant flexibility to reach the partially unfolded state. More importantly, there are six hydrophobic clusters with the maximal hydrophobicity around the residues C6, W28, L56, L83, W108, and

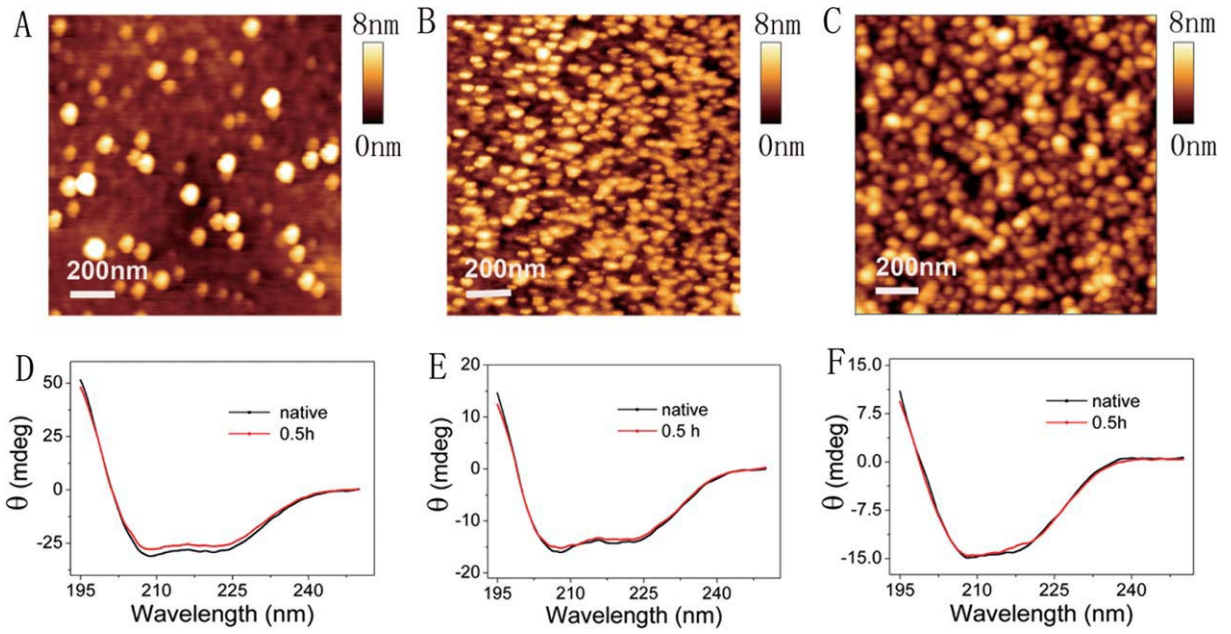

Figure 9

The morphology of the protein aggregates on 0.5 h UV illumination, (**A**) BSA, (**B**) α-Lactalbumin, and (**C**) RNase A, respectively. The Far-UV CD spectra of the illuminated structures and their corresponding native ones of proteins, (**D**) BSA, (**E**) α-Lactalbumin, and (**F**) RNase A, respectively. The protein samples (2.0 mg/mL) are illuminated for 0.5 h at pH 7. Note that intensity of UV doses is 200 μW/cm^2 for BSA and Bovine α-Lactalbumin and is 500 μW/cm^2 for protein RNase A.

W123, respectively in CEWL.[33–38] In the native CEWL, these hydrophobic residues are largely stabilized and protected by the four native disulfide bonds. After the rupture of some of the disulfide bonds, these hydrophobic clusters can be easily exposed to the solvent in the partially unfolded states. Such unique features of the partially unfolded CEWL under UV illumination allow the hydrophobic aggregation and disulfide bonding to be two major driving forces for the aggregation process. We envision that it is possible to control the breakage of the disulfide bonds in CEWL by changing the intensity of the UV light. This can lead to a distinct balance between the hydrophobic collapse and disulfide bonding and subsequently change the morphology of the assemblies.

To reveal whether such aggregation mechanism is general among disulfide-bonded proteins, we applied UV illumination to three additional disulfide-bonded proteins, BSA, α-lactalbumin, and RNase A. As shown in Figure 9(A–C), all these three proteins can assemble into globular aggregates under UV illumination at a concentration of 2 mg/mL, the same as that of lysozyme. Moreover, for all three proteins, their secondary structures are largely maintained after 30-min illumination [Fig. 9(D–F)], which is similar to the case of CEWL. This indicates that formation of partially unfolded structures is indeed a general mechanism for the formation of ordered globular aggregates. However, due to their intrinsic properties (e.g., number of disulfide bonds, photo sensitive amino acid tryptophan and tyrosine, and solvent exposed hydrophobic residues on rupture of disulfide bonds), the amount and size of the globular aggregates for these three proteins are different from that of lysozyme [Fig. 9(A–C)]. Note that the excitation of tyrosine in proteins may also play important roles in the rupture of disulfide bonds. A direct evidence for this comes from the aggregation of RNase A on UV illumination, as it contains five tyrosine residues but no tryptophan. However, to rupture disulfide bonds through tyrosine based photochemical process, much elevated UV doses are required.[26] We only observed aggregation of RNase A at the intensity of UV illumination 2.5 times stronger than the other three proteins studied in this work. At the UV intensity similar to that for the study of other three proteins, we did not observe any aggregation even after illumination for 2 h. The interesting aggregation behaviors of these disulfide-bonded proteins warrant further detailed studies of their unique aggregation mechanism.

CONCLUSION

In this work, we report that protein CEWL can self-assemble into granular aggregates and subsequently globule-like aggregates in native condition under continuous UV illumination. We studied the mechanism that governs this aggregation process. UV illumination reduces the

native disulfide bonds in CEWL via a photochemical process that leads to partially unfolding of CEWL. Such an unfolded state is metastable with exposed hydrophobic residues and free thiols. They gradually aggregate into granules in the initial stage by the formation of intermolecular hydrophobic interactions. This process is kinetically slow because the partially unfolded CEWL still retain certain stability, hindering the formation of intermolecular disulfide bonds. Thus, the aggregates show granular structure instead of amorphous macroscopic aggregates or amyloid-like fibrils with β-structures. These granules are highly reactive and can further grow into larger globular aggregates dominated by both the hydrophobic interactions and the intermolecular disulfide bonds with longer illumination time or prolonged incubation. Thus, as UV illumination from sun light is inevitable in our daily life, our study points out the potential danger of the over-exposure to sun light as it may cause the partially unfolding and even aggregation of some proteins. Deciphering the aggregation mechanism of the partially unfolded proteins will be the first step toward the understanding of the pathological consequences of these aggregates.

REFERENCES

1. Anfinsen CB. Principles that govern the folding of protein chains. Science 1973;181:223–230.
2. Mayor U, Guydosh NR, Johnson CM, Grossmann JG, Sato S, Jas GS, Freund SM, Alonso DO, Daggett V, Fersht AR. The complete folding pathway of a protein from nanoseconds to microseconds. Nature 2003;421:863–867.
3. Wolynes PG, Onuchic JN, Thirumalai D. Navigating the folding routes. Science 1995;267:1619–1620.
4. Dill KA, Chan HS. From Levinthal to pathways to funnels. Nat Struct Biol 1997;4:10–19.
5. Sasahara K, Yagi H, Naiki H, Goto Y. Heat-induced conversion of beta(2)-microglobulin and hen egg-white lysozyme into amyloid fibrils. J Mol Biol 2007;372:981–991.
6. Hwang H, Choi H, Kim HK, Jo do H, Kim TD. Ionic liquids promote amyloid formation from alpha-synuclein. Anal Biochem 2009;386:293–295.
7. Vernaglia BA, Huang J, Clark ED. Guanidine hydrochloride can induce amyloid fibril formation from hen egg-white lysozyme. Biomacromolecules 2004;5:1362–1370.
8. Calloni G, Lendel C, Campioni S, Giannini S, Gliozzi A, Relini A, Vendruscolo M, Dobson CM, Salvatella X, Chiti F. Structure and dynamics of a partially folded protein are decoupled from its mechanism of aggregation. J Am Chem Soc 2008;130:13040–13050.
9. Radford SE, Dobson CM. From computer simulations to human disease: emerging themes in protein folding. Cell 1999;97:291–298.
10. Rochet JC, Lansbury PT, Jr. Amyloid fibrillogenesis: themes and variations. Curr Opin Struct Biol 2000;10:60–68.
11. Thomas PJ, Qu BH, Pedersen PL. Defective protein folding as a basis of human disease. Trends Biochem Sci 1995;20:456–459.
12. Dobson CM. Getting out of shape. Nature 2002;418:729–730.
13. Goedert M. Alpha-synuclein and neurodegenerative diseases. Nat Rev Neurosci 2001;2:492–501.
14. Kelly JW. The alternative conformations of amyloidogenic proteins and their multi-step assembly pathways. Curr Opin Struct Biol 1998;8:101–106.
15. Uversky VN. Alpha-synuclein misfolding and neurodegenerative diseases. Curr Protein Pept Sci 2008;9:507–540.
16. Klein WL, Krafft GA, Finch CE. Targeting small Abeta oligomers: the solution to an Alzheimer's disease conundrum? Trends Neurosci 2001;24:219–224.
17. Lambert MP, Barlow AK, Chromy BA, Edwards C, Freed R, Liosatos M, Morgan TE, Rozovsky I, Trommer B, Viola KL, Wals P, Zhang C, Finch CE, Krafft GA, Klein WL. Diffusible, nonfibrillar ligands derived from Abeta1-42 are potent central nervous system neurotoxins. Proc Natl Acad Sci USA 1998;95:6448–6453.
18. Walsh DM, Klyubin I, Fadeeva JV, Cullen WK, Anwyl R, Wolfe MS, Rowan MJ, Selkoe DJ. Naturally secreted oligomers of amyloid beta protein potently inhibit hippocampal long-term potentiation in vivo. Nature 2002;416:535–539.
19. Conway KA, Lee SJ, Rochet JC, Ding TT, Williamson RE, Lansbury PT, Jr. Acceleration of oligomerization, not fibrillization, is a shared property of both alpha-synuclein mutations linked to early-onset Parkinson's disease: implications for pathogenesis and therapy. Proc Natl Acad Sci USA 2000;97:571–576.
20. Tompkins MM, Hill WD. Contribution of somal Lewy bodies to neuronal death. Brain Res 1997;775:24–29.
21. Neves-Petersen MT, Gryczynski Z, Lakowicz J, Fojan P, Pedersen S, Petersen E, Petersen SB. High probability of disrupting a disulphide bridge mediated by an endogenous excited tryptophan residue. Protein Sci 2002;11:588–600.
22. Wu L-Z, Sheng Y-B, Xie J-B, Wang W. Photoexcitation of tryptophan groups induced reduction of disulfide bonds in hen egg white lysozyme. J Mol Struct 2008;882:101–106.
23. Prompers JJ, Hilbers CW, Pepermans HA. Tryptophan mediated photoreduction of disulfide bond causes unusual fluorescence behaviour of Fusarium solani pisi cutinase. FEBS Lett 1999;456:409–416.
24. Vanhooren A, Devreese B, Vanhee K, Van Beeumen J, Hanssens I. Photoexcitation of tryptophan groups induces reduction of two disulfide bonds in goat alpha-lactalbumin. Biochemistry 2002;41:11035–11043.
25. Neves-Petersen MT, Snabe T, Klitgaard S, Duroux M, Petersen SB. Photonic activation of disulfide bridges achieves oriented protein immobilization on biosensor surfaces. Protein Sci 2006;15:343–351.
26. Neves-Petersen MT, Klitgaard S, Pascher T, Skovsen E, Polivka T, Yartsev A, Sundstrom V, Petersen SB. Flash photolysis of cutinase: identification and decay kinetics of transient intermediates formed upon UV excitation of aromatic residues. Biophys J 2009;97:211–226.
27. Petersen SB, Kold di Gennaro A, Neves-Petersen MT, Skovsen E, Parracino A. Immobilization of biomolecules onto surfaces according to ultraviolet light diffraction patterns. Appl Opt 2010;49:5344–5350.
28. Cao A, Hu D, Lai L. Formation of amyloid fibrils from fully reduced hen egg white lysozyme. Protein Sci 2004;13:319–324.
29. Chiti F, Dobson CM. Amyloid formation by globular proteins under native conditions. Nat Chem Biol 2009;5:15–22.
30. Camacho CJ, Thirumalai D. Modeling the role of disulfide bonds in protein folding: entropic barriers and pathways. Proteins 1995;22:27–40.
31. Indu S, Kochat V, Thakurela S, Ramakrishnan C, Varadarajan R. Conformational analysis and design of cross-strand disulfides in antiparallel beta-sheets. Proteins 2011;79:244–260.
32. Indu S, Kumar ST, Thakurela S, Gupta M, Bhaskara RM, Ramakrishnan C, Varadarajan R. Disulfide conformation and design at helix N-termini. Proteins 2010;78:1228–1242.
33. Schwalbe H, Fiebig KM, Buck M, Jones JA, Grimshaw SB, Spencer A, Glaser SJ, Smith LJ, Dobson CM. Structural and dynamical properties of a denatured protein. Heteronuclear 3D NMR experiments and theoretical simulations of lysozyme in 8 M urea. Biochemistry 1997;36:8977–8991.
34. Miranker A, Radford SE, Karplus M, Dobson CM. Demonstration by NMR of folding domains in lysozyme. Nature 1991;349:633–636.
35. Radford SE, Dobson CM, Evans PA. The folding of hen lysozyme involves partially structured intermediates and multiple pathways. Nature 1992;358:302–307.
36. Klein-Seetharaman J, Oikawa M, Grimshaw SB, Wirmer J, Duchardt E, Ueda T, Imoto T, Smith LJ, Dobson CM, Schwalbe H. Long-

range interactions within a nonnative protein. Science 2002; 295:1719–1722.
37. Mishima T, Ohkuri T, Monji A, Imoto T, Ueda T. A particular hydrophobic cluster in the residual structure of reduced lysozyme drastically affects the amyloid fibrils formation. Biochem Biophys Res Commun 2007;356:769–772.
38. Wirmer J, Schlorb C, Klein-Seetharaman J, Hirano R, Ueda T, Imoto T, Schwalbe H. Modulation of compactness and long-range interactions of unfolded lysozyme by single point mutations. Angew Chem Int Ed Engl 2004;43:5780–5785.
39. Goldberg ME, Semisotnov GV, Friguet B, Kuwajima K, Ptitsyn OB, Sugai S. An early immunoreactive folding intermediate of the tryptophan synthease beta 2 subunit is a 'molten globule'. FEBS Lett 1990;263:51–56.
40. Shih P, Holland DR, Kirsch JF. Thermal stability determinants of chicken egg-white lysozyme core mutants: hydrophobicity, packing volume, and conserved buried water molecules. Protein Sci 1995;4:2050–2062.
41. Wetter LR, Deutsch HF. Immunological studies on egg white proteins. IV. Immunochemical and physical studies of lysozyme. J Biol Chem 1951;192:237–242.
42. van den Berg B, Chung EW, Robinson CV, Mateo PL, Dobson CM. The oxidative refolding of hen lysozyme and its catalysis by protein disulfide isomerase. EMBO J 1999;18:4794–4803.
43. Ellman GL. Tissue sulfhydryl groups. Arch Biochem Biophys 1959; 82:70–77.
44. Wang C, Chen S, Wang X, Wang L, Wallis AK, Freedman RB, Wang CC. Plasticity of human protein disulfide isomerase: evidence for mobility around the X-linker region and its functional significance. J Biol Chem 2010;285:26788–26797.
45. Goda S, Takano K, Yamagata Y, Nagata R, Akutsu H, Maki S, Namba K, Yutani K. Amyloid protofilament formation of hen egg lysozyme in highly concentrated ethanol solution. Protein Sci 2000;9:369–375.
46. Krebs MR, Wilkins DK, Chung EW, Pitkeathly MC, Chamberlain AK, Zurdo J, Robinson CV, Dobson CM. Formation and seeding of amyloid fibrils from wild-type hen lysozyme and a peptide fragment from the beta-domain. J Mol Biol 2000;300:541–549.
47. Arnaudov LN, de Vries R. Thermally induced fibrillar aggregation of hen egg white lysozyme. Biophys J 2005;88:515–526.
48. Shashilov VA, Lednev IK. 2D correlation deep UV resonance raman spectroscopy of early events of lysozyme fibrillation: kinetic mechanism and potential interpretation pitfalls. J Am Chem Soc 2008;130:309–317.
49. Dumoulin M, Kumita JR, Dobson CM. Normal and aberrant biological self-assembly: Insights from studies of human lysozyme and its amyloidogenic variants. Acc Chem Res 2006;39:603–610.
50. Booth DR, Sunde M, Bellotti V, Robinson CV, Hutchinson WL, Fraser PE, Hawkins PN, Dobson CM, Radford SE, Blake CC, Pepys MB. Instability, unfolding and aggregation of human lysozyme variants underlying amyloid fibrillogenesis. Nature 1997; 385:787–793.
51. Petersen MT, Jonson PH, Petersen SB. Amino acid neighbours and detailed conformational analysis of cysteines in proteins. Protein Eng 1999;12:535–548.